

DEVELOPMENT OF HIGH CURRENT CYCLOTRON AND ASSOCIATED BEAM DYNAMICS STUDIES AT VECC

V. S. Pandit

Variable Energy Cyclotron Centre, 1- AF, Bidhannagar, Kolkata-700 064, India

Abstract

In this paper we present the results of simulation works carried out to settle some of the technical and physics issues related with the injection and acceleration of space charge dominated beam in a compact cyclotron. The design issues of injection system and various subsystems and some new results of simulation studies on magnet design using random search technique, space charge effect on beam bunching and behaviour of beam envelope in the central region etc. are reported. The operating experience and current status of the 2.45 GHz microwave ion source and low energy beam transport system has also been discussed.

INTRODUCTION

A 10 MeV, 5 mA four sector compact cyclotron for proton is under development at VECC Kolkata. Proton beam at 100 keV from 2.45 GHz microwave ion source (under testing for performance improvement) will be first collimated and bunched [1]. It will be injected axially in the central region where a spiral inflector will place the beam on the proper orbit. Two delta type resonators located in the opposite valleys will be used to accelerate the beam. At the final energy beam will be extracted using an electrostatic deflecting channel. The main aim of this injector cyclotron project is to study and settle various physics and technological problems associated with the production, bunching, acceleration, injection, extraction, etc. of the high intensity proton beams [2, 3].

PARAMETERS OF THE CYCLOTRON

We have chosen the configuration of the magnet having four sectors with maximum magnetic field of 1.5T at the hill centre. A deep valley structure is used to provide strong focusing in the vertical direction i.e. vertical betatron tune $\nu_z > 0.5$ at all radii. This is necessary for handling the space charge defocusing force at an average beam current of ~ 5 mA. The hill gap is 5 cm and the valley gap is 50 cm, same as the distance between the upper and lower return yokes. For the injection system, one hole is provided at the center. Eight more holes in the four valleys are provided for vacuum pumps and rf cavities. Apart from using a high dee voltage (125 kV), a very low average magnetic field ~ 0.689 T is chosen to get large extraction radius of ~ 65 cm for 10 MeV compact cyclotron [4, 5]. This helps to have a reasonable turn separation at the extraction radius to get loss free extraction of the beam. In order to meet the isochronisms, the shaping of the azimuthally averaged magnetic field was done with the help of varying the sector angular width along the radius.

In general the magnet pole shimming is an iterative process [6, 7]. We have developed a shimming method, which gives smooth sector geometry of the hill. We have approximated the shape of the sector by a polynomial function of the radius and minimized the frequency error by optimizing the coefficients of the polynomial using random search technique. For details see reference [8].

We have used a 3D magnetic field code MagNet [9] to calculate the field in the median plane and obtained the frequency errors as a function of energy using equilibrium orbit code GENSPEO [10]. These frequency errors are then minimized by modifying the sector geometry. Proper symmetry considerations allowed us to use only 1/16 portion of the magnet (see Fig. 1).

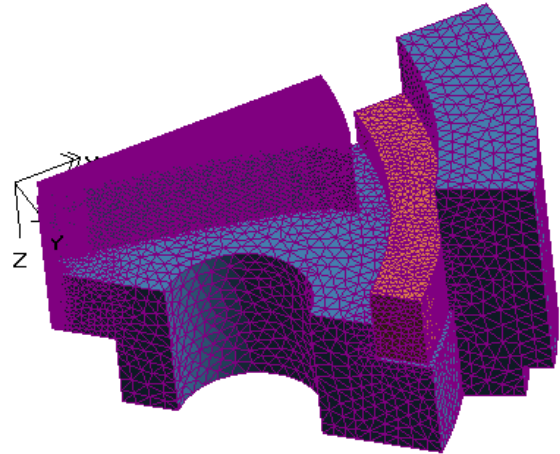


Figure 1: Model of the magnet with mesh.

Table 1: Parameters of the 10MeV cyclotron

Injection energy	100 keV/80keV
Final energy	10 MeV
Injection radius	6.6 cm
Hill field B_H /Valley field B_V	1.5 T/1.5 T
Pole gap Hill /Valley	5 cm / 50 cm
Hill angle min. / max.	$33.8^\circ / 34.2^\circ$
Number of resonators	2 delta type, 45°
RF frequency	42 MHz
Harmonic no.	4
RF Voltage inj. /ext.	125 kV / 150kV
Phase width	30°
Radial tune ν_r	1.1 - 1.2
Vertical tune ν_z	0.61 - 0.99
Effective turn separation	6mm @5mA
Limiting current TSC / LSC	15mA/ 13mA

The radial and axial tunes, integrated phase shift etc. were found out for the optimized sector shape using the equilibrium orbit program as shown in Figure 4. The phase excursion in the entire region is limited within $\pm 2^\circ$. We have also checked the centering of the accelerated orbits using the optimized magnetic field data. The electric field E in the accelerating gaps of the two resonators has been approximated by a Gaussian function. Figure 5 shows the position of the accelerating gaps (G-1 to G-4) in the median plane and accelerated orbits of proton up to the extraction radius.

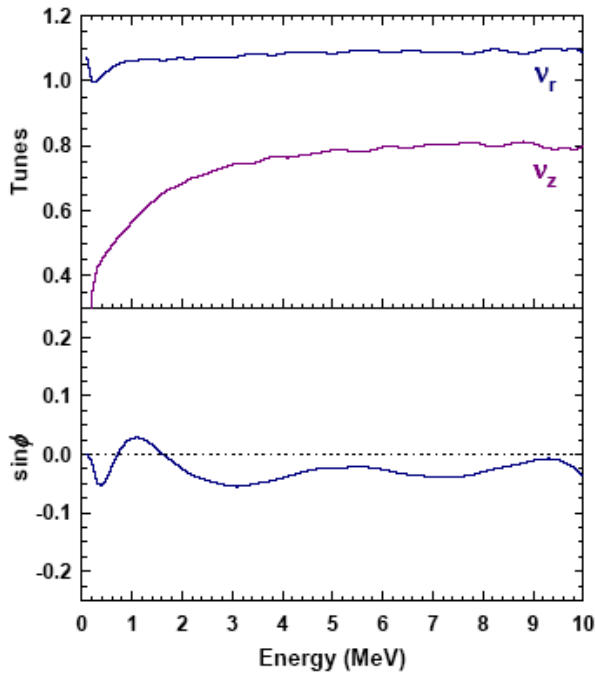


Figure 4: Variation of betatron tunes and phase slip $\sin\phi$ as a function of energy obtained using random search optimisation technique.

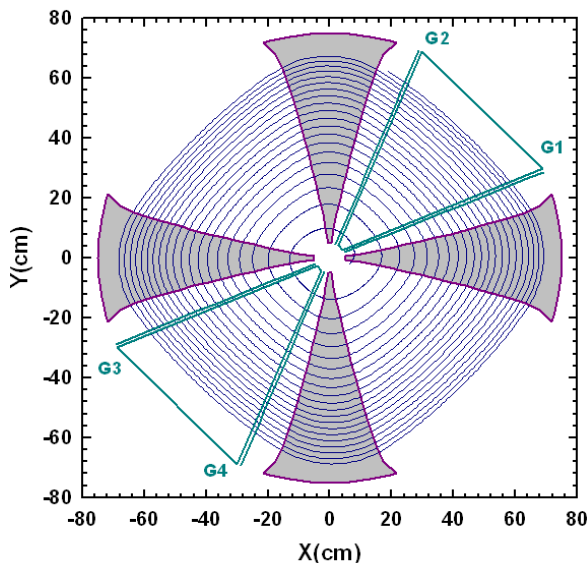


Figure 5: Location of the accelerating gaps and optimised accelerated orbits for proton from 100 keV to 10 MeV.

ION SOURCE AND INJECTION SYSTEM

Ion Source consists of a plasma chamber, two movable solenoids to produce desired axial magnetic field and the triode ion extraction system. The diameter of the apertures in the plasma, accelerating and de-accelerating electrodes is 6mm, 8mm and 8 mm respectively. The plasma chamber is a double walled water-cooled cylindrical stainless steel chamber of 100 mm length and 90 mm diameter. The microwave power from the 2.45 GHz, 1.2kW magnetron is coupled through a three stubs tuning unit, an autotuner and a ridged wave-guide. Ion source along with adjustable solenoids, its power supplies, microwave generator, gas cylinder and a high precision gas flow system etc., all are kept at 100kV high voltage deck. Deck is isolated from the ground through polypropylene insulators. A two-segment ceramic insulators (Al_2O_3) column, which supports the beam extraction electrodes, isolates the high voltage deck and the beam line at the ground potential. Power to the various subsystems on the deck is supplied using a 150kV, 30kW isolation transformer.

The injection beam line consists of two magnetic solenoids (SOL1: 40cm, 3.6kG) (SOL2: 40cm, 3.3kG), adjustable slits, faraday cup and profile monitoring box. The beam from the ion source is expected to contain a substantial fraction (~ 10 to 20 %) of molecular hydrogen ion. We have provided a slit at the waist position of the proton beam after the first solenoid to reject most of the molecular hydrogen beam. Beam current measuring equipments used in the beam line are; a water-cooled faraday cup (up to 10mA only) with secondary electron suppresser and a DCCT. We have used three turbo pumps each having pumping speed of 520 l/s to evacuate the entire system. A pressure of the order of 3.5×10^{-7} mbar has been achieved in the beam line. Control system of the source parameters such as adjusting the current in the solenoids, movement of solenoids, tuning of microwave power, adjustment of gas flow etc. is placed on the high voltage deck and adjustment and monitoring is done with a PC at ground potential through optical fiber.

Initial promising operations were halted several times due to failure of the electronic components at the high voltage deck and problem in microwave coupling. There was lots of heating in the ridged wave-guide. Controls of various devices and of manual tuner of microwave at the HV deck did not work properly. We inserted an auto tuner in the system. A new water-cooled ridged wave-guide was designed, fabricated to replace the existing one. We faced lots of glow discharge and internal arcing during initial operation in the extraction region. We are planning to add some iron sheets in the extraction region to reduce the magnetic field in the extraction zone. Our operation was halted several times due to the thermal fracture of microwave window from the back streaming electrons and source plasma heating. In order to protect the microwave window from back streaming electron we have now placed a 5 mm thick boron nitride plate behind the water-cooled plasma chamber.

Ion Source is presently under testing for performance improvement. We have already extracted 8.5 mA proton beam near the extraction (measured by DCCT) and 6.4 mA (after collimation by a 1cm x 1cm slit) at the faraday cup 1.5m away from the extraction at an extraction voltage of 80kV. We transported this beam up to the last beam dump near the diagnostic chamber and observe the beam on water cooled alumina plate.

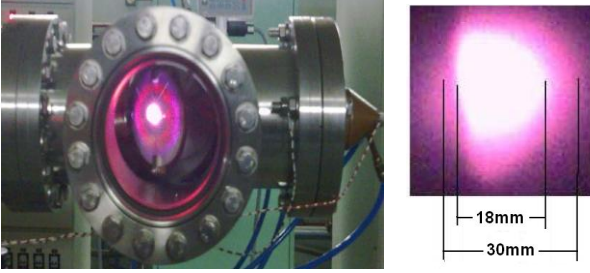


Figure 4: Beam spot of 80keV, 5 mA proton on water cooled alumina plate placed at the end of beam line near beam dump.

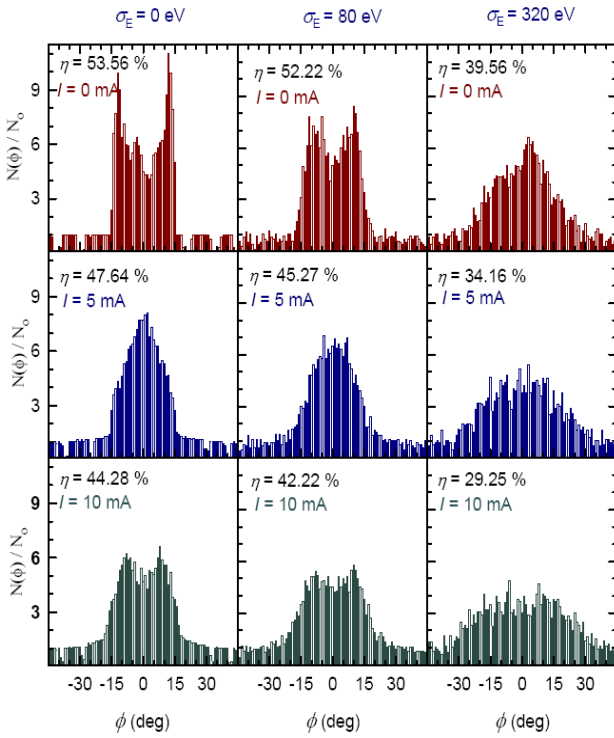


Figure 5: Relative density distribution of discs at the time focus as a function of phase ϕ for 100 keV beam at current $I = 0$ mA ($L = 100$ cm), $I = 5$ mA ($L = 87$ cm) and $I = 10$ mA ($L = 79$ cm) and for three different values of initial beam energy spread (column 1 for $\sigma_E = 0$ eV, column 2 for $\sigma_E = 80$ eV and column 3 for $\sigma_E = 320$ eV). Large energy spread together with space charge affects the bunching action adversely.

Buncher Simulation

The extracted beam from the ion source will be bunched using a sinusoidal buncher (expected bunching efficiency is $\sim 40\%$ for space charge dominated beam) and

will be injected axially in the central region of the cyclotron where a spiral inflector will place the beam on the proper orbit. We have carried out detailed simulation of the beam bunching for a sinusoidal buncher using disk model to incorporate the space charge effects. Simulation results show that at high current, space charge forces affect the bunching efficiency and put restrictions on the distance L of the buncher from the time focus. The bunching efficiency is also found to decrease. The influence of the space-charge effect can be compensated, to some extent, by using slightly higher bunching voltage. We have also studied the effect of energy spread on beam bunching. A detail of the beam bunching system and simulation method is described in reference [11].

Spiral Inflector

As mentioned earlier a spiral inflector will deflect the beam in the median plane of the 10 MeV cyclotron and place the beam on the proper orbit. We have studied the various optical properties of the inflector in the presence of space charge effects. We have included a space charge term in the paraxial trajectory equations assuming long cylindrical beam with uniform density. The analysis was done for 50 mA peak beam current (which corresponds to ~ 5 mA average current) with radial width ± 4 mm and divergences ± 18 mrad at the inflector entrance and optimization was done on the input starting conditions of the beam to get the desired output beam properties with minimum coupling effects.

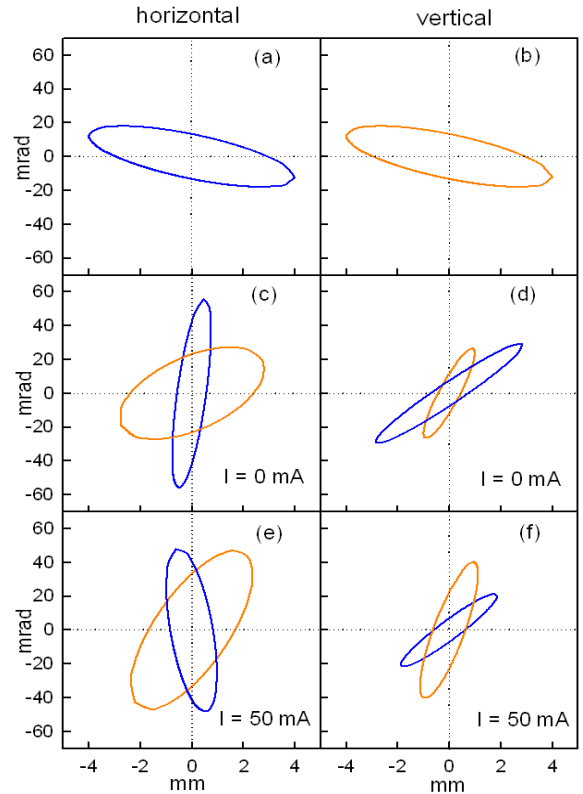


Figure 6: Phase space diagram in both planes. a) & b) for entrance; c) & d) at exit for 0 mA beam current; e) & f) at exit for 50 mA beam current for optimised input ellipse.

In calculations we have considered 40 particles that belong to the boundary of the contours in (u - p_u) and (h - p_h) planes and correspond to the optimized ellipse of 53.33π mmrad at the entrance of the inflector. The phase ellipses, in both planes at the entrance and exit for 0 mA and 50 mA of beam current for optimized conditions are presented in Figure 6. The estimated effective emittances at the exit in the horizontal and vertical planes are approximately equal to 86π mmrad and 32π mmrad respectively for 50 mA beam current. We observed that the influence of space charge is drastic on emittance growth with upright ellipse as initial conditions. However, by using optimized tilted ellipse the emittance growth is minimal. Thus the optimization for matching is very much important. This inflector has already been fabricated and tested in vacuum up to 25 kV. Soon it will be tested with beam. We have worked out the injection scheme at 100keV as well as at 80keV.

Central region study

We have also done some studies on the central region to optimise the central plug position and check the centering errors with the above spiral inflector. The input parameters used are following: Injection energy 100keV, Dee Voltage 125kV, gap width between dee and dummy-dee 2cm, dee height 3cm and magnetic field data from the 3D code. A Gaussian distribution function was used for the electric field in the four accelerating gaps. The central trajectories as well as radial and axial beam envelopes along the accelerated orbit for two different values of beam current have been studied. The maximum vertical displacement from the median plane is found to be less than 4 mm for 5mA of beam current. The vertical height of the dee from the median plane is 15mm. The vertical focussing that is achieved by properly adjusting the geometry and the phase of rf plays a crucial role for control of beam loss in the vertical direction. Figure 7 shows the beam envelopes in radial and axial direction along the accelerated orbit (shown in Fig 5). A detailed investigation reveals that amplitude growth and oscillation in the horizontal beam envelope is very sensitive to the radial betatron tune ν_r . The contributions from ellipse orientation, inter plane coupling and space charge effects are comparatively small on these oscillations. A slight change in ν_r above or below the present value reduces the amplitude growth as well as oscillation by large amount. We feel that this phenomenon is due to the fact that ν_r is very close to the resonance $\nu_r = 1$. Our estimation shows that 5 mA beam can be easily controlled within the 5mm of beam radius in the present design of the cyclotron.

CONCLUSION

In this paper we have discussed the efforts put at VECC on the development of 2.45GHz microwave ion source and injection system. We have discussed the results of simulation including the space charge effects carried on 10MeV, 5mA compact cyclotron.

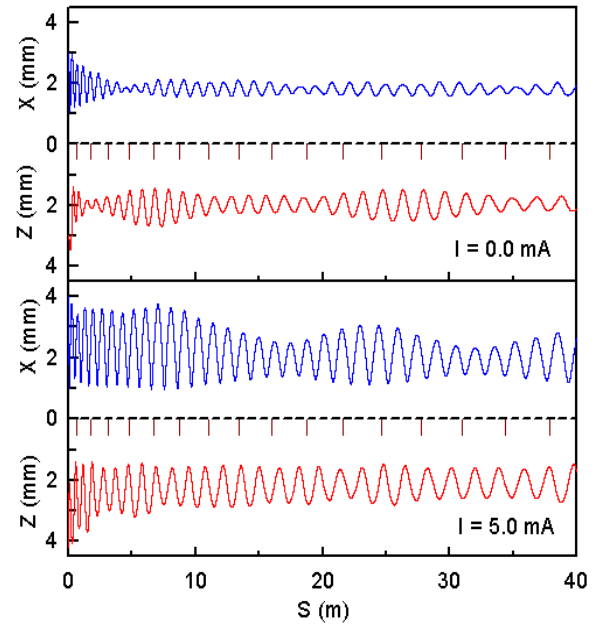


Figure 7: Radial (X) and axial (Z) beam envelopes along the accelerated orbit. The value of initial normalised beam emittance $\epsilon_n=0.8\pi$ mmmrad in both the planes.

ACKNOWLEDGEMENT

The work presented here is done by a team consisting of Sri G. Pal, P. Sing Babu, Animesh Goswami, R. C. Yadav, S. Bhattacharya, S. Srivastava, Mou Chatterjee, A. Misra, and P. R. Sarma.

REFERENCES

- [1] V. S. Pandit, Indian Particle Accelerator Conference InPAC-05 (2005) 13
- [2] N. Fieuer and P. Mandrillon; Proc. of the 14th Int. Conf. on Cyclotrons and their Applications, Cape Town, (1995) 598.
- [3] Th. Stammbach, S. Adam, H. R. Fitze, W. Joho, M. Marki, M. Olivo, L. Rezzonico, P. Sigg and U. Schryber; Nucl. Instr. and Meth. B 113 (1996) 1
- [4] V. S. Pandit and P. S. Babu; Nucl. Instr. and Meth. A **523** (2004) 19.
- [5] A. Goswami, P. Sing Babu and V. S. Pandit; Nucl. Instr and Meth. A **562** (2006) 34.
- [6] V. S. Pandit, P. Sing Babu, A. Goswami, P. R. Sarma; 4th Asian Particle Accelerator Conference, APAC-2007, 342.
- [7] B. Qin, D. Z.Chen, L. C. Zhao, J. Yang, M. W. Fan, Nucl. Instr. and Meth. A620 (2010) 121.
- [8] P. Sing Babu A. Goswami, P. R. Sarma, V. S. Pandit; Nucl. Instr. and Meth. A **624** (2010) 560.
- [9] MagNet User Guide, Infolytica Corporation.
- [10] M. M. Gordon, Particle Accelerators, **16** (1984) 39.
- [11] P. Sing Babu A. Goswami, and V. S. Pandit; Nucl. Instr. and Meth. A **603** (2009) 222.